



MIT Open Access Articles

Stratigraphic correlation and splice generation for sediments recovered from a large-lake drilling project: an example from Lake Junín, Peru

The MIT Faculty has made this article openly available. **Please share** how this access benefits you. Your story matters.

As Published	https://doi.org/10.1007/s10933-019-00098-w
Publisher	Springer Netherlands
Version	Author's final manuscript
Citable link	https://hdl.handle.net/1721.1/131744
Terms of Use	Article is made available in accordance with the publisher's policy and may be subject to US copyright law. Please refer to the publisher's site for terms of use.

Stratigraphic correlation and splice generation for sediments recovered from a large-lake drilling project: an example from Lake Junín, Peru

Cite this article as: R. G. Hatfield, A. Woods, S. B. Lehmann, N. Weidhaas, C. Y. Chen, M. B. Abbott, D. T. Rodbell and J. S. Stoner, Stratigraphic correlation and splice generation for sediments recovered from a large-lake drilling project: an example from Lake Junín, Peru, *Journal of Paleolimnology* <https://doi.org/10.1007/s10933-019-00098-w>

This Author Accepted Manuscript is a PDF file of an unedited peer-reviewed manuscript that has been accepted for publication but has not been copyedited or corrected. The official version of record that is published in the journal is kept up to date and so may therefore differ from this version.

Terms of use and reuse: academic research for non-commercial purposes, see here for full terms. <https://www.springer.com/aam-terms-v1>

Author accepted manuscript

Stratigraphic correlation and splice generation for sediments recovered from a large-lake drilling project: an example from Lake Junín, Peru

Hatfield, R.G.^{1,2*}, Woods, A.³, Lehmann, S.B.³, Weidhaas, N.³, Chen, C.Y.⁴, Abbott, M.B.³, Rodbell, D.T.⁵, and Stoner, J.S.¹

¹ College of Earth, Ocean, and Atmospheric Science, Oregon State University, Corvallis, OR 97330, USA

² Department of Geological Sciences, University of Florida, Gainesville, FL 32611, USA

³ Geology and Environmental Science, University of Pittsburgh, PA 15260, USA

⁴ Department of Earth, Atmospheric, and Planetary Sciences, Massachusetts Institute of Technology, Cambridge, MA 02139, USA

⁵ Department of Geology, Union College, Schenectady, NY 12308, USA

* corresponding author: rhatfield1@ufl.edu

Key words:

Stratigraphic correlation; Splice; ICDP; Sediment cores; Depth scale; Lake Junín

Author accepted manuscript

Abstract

Sediment records from deep-drilling projects such as those carried out by the International Continental Scientific Drilling Program (ICDP) are often tens- to hundreds-of-meters in length. To ensure the complete recovery of a stratigraphic section, a basin is usually cored multiple times in adjacent holes so that gaps between sequential cores, poorly-recovered sections, or intervals affected by disturbance can be bridged or replaced with sediments from another hole. Stratigraphic correlation, the alignment of stratigraphically-equivalent horizons in cores from different holes in a common-depth scale, and splice generation, the integration of the most-representative core sections into a composite-stratigraphic section, are essential steps in this process to both evaluate and synthesize the recovered-sediment record and focus the scientific analyses. However, these undertakings can be complex and are inherently subjective, making the need for the development of a single robust stratigraphic section early in the project critical to its success. Despite this, the steps between core recovery and on-splice data generation are rarely published in sufficient detail to allow reconstruction, or refinement, of the composited record at a later date. To increase the transparency of how the composite record is created, and to provide a template for future projects, we detail the step-by-step approaches and decisions involved in generating the composite-depth scale and complete-stratigraphic splice following recovery of sediments from Lake Junín, Peru. We first explain the details and nuances of different drilling-depth scales before describing how we integrated different physical property records to generate the composite-depth scale and complete-stratigraphic splice. Here, we show that due to the complex stratigraphy in the Lake Junín sediments, high-resolution line-scan images of the cores offer millimeter-scale precision for construction of the primary-stratigraphic splice at a resolution not afforded by other physical-property data. Finally, through comparison of the spliced record to physical-property records acquired *in-situ* on the borehole, we demonstrate that the stratigraphic splice is an accurate representation of the sediment accumulated in the Lake Junín basin.

Introduction

Much of our knowledge about the variability in Earth's natural systems such as global temperature (Zachos et al. 2001; Elderfield et al. 2012), ocean-circulation patterns (Praetorius et al. 2008; Hernández-Molina et al. 2014), ice-sheet growth and (in)stability (Blake-Mizen et al., 2019; Larsen et al., 1994), geomagnetic behavior (Stoner et al. 2013; Channell et al. 2016), and arctic (Melles et al. 2012; Barker et al. 2015) and tropical (Herbert et al. 2010; Zhang et al. 2014) climate has been derived from multi-core, multi-hole, deep drilling projects such as those carried out by the International Ocean Discovery Program (IODP) and International Continental Scientific Drilling Program (ICDP). The success of these programs has resulted from their ability to couple deep-drilling technologies with high rates of sediment recovery to generate long-continuous-sediment records. However, the development of a complete- and continuous-sedimentary section is not always straightforward. For example, subtle differences in sediment accumulation and stratigraphy can result in variability between cores recovered from adjacent holes, while coring artifacts, such as incomplete recovery, disturbance, and/or sediment stretching and squeezing, can affect the quality of the recovered sediments. Even if these factors are negligible and sediment recovery approaches 100%, a continuous stratigraphic record cannot be obtained from a single hole due to gaps between successive cores (Ruddiman et al. 1987). The most common approach to circumvent these issues is to recover multiple copies of the stratigraphy at a site from several different holes and then to combine them to generate a complete- and representative-stratigraphic section. This is accomplished via two-main steps: sediments from different holes are first mapped into a common-depth scale through correlation of equivalent stratigraphic features, and then the most representative sediment sections are spliced together to form a continuous record, or "splice" (Ruddiman et al. 1987; Hagelberg et al. 1995).

The stratigraphic splice is often considered the best representation of the sediment accumulated at any given site. This record is frequently the target for the majority of sample requests and is the basis for development of the primary-age model. On IODP expeditions and many ICDP projects, an initial composite-depth scale is often generated at sea or in the field to inform drilling decisions in real time and to ensure complete recovery of the sequence (Ruddiman et al. 1987). The necessity for rapid data acquisition means that these records are usually constructed using physical properties, such as magnetic susceptibility (MS), gamma ray attenuation (GRA), and/or natural gamma radiation (NGR) measured at relatively-low resolution (centimeter- to decimeter-intervals) acquired on

whole (unsplit) core sections. As a result, it is often necessary to revisit, validate, and refine field-generated-composite-depth records in the laboratory with additional data in order to develop a robust-stratigraphic splice. For IODP expeditions, the shipboard-stratigraphic correlation and splice for each site is detailed in a dedicated sub-chapter in the expedition Proceedings volume, and shore-based revisions, which are commonplace in paleoceanographic- and paleoclimatic-focused projects, are frequently published in journals or as updates in data reports (Hagelberg et al. 1995; Evans et al. 2004; Wilkens et al. 2013; Hatfield 2015; van Peer et al. 2017). In contrast, results from deeply-drilled lake and terrestrial projects often go unreported or the existence of a composite section is only briefly acknowledged in initial publications before the discussion moves onto the stratigraphy and/or age-model results (Melles et al. 2011; Scholz et al. 2011; Litt et al. 2012; Kliem et al. 2013). Moreover, because the generation of composite-depth scales and splices are inherently subjective endeavors, a lack of transparency often makes it difficult to reconstruct, or if necessary refine, the composite-depth scale and/or splice if issues arise at a later date.

In this manuscript, we focus on detailing the steps taken and issues encountered in producing the composite-depth record and stratigraphic splice from Lake Junín, Peru. We adopt an IODP style approach to stratigraphic correlational and in many ways the sediments recovered from Lake Junín are typical of those recovered during IODP expeditions (e.g., multiple-hole, multiple-core recovery). However, as Lake Junin's stratigraphy is more complex than most marine sediment sequences, and as we integrate sediments recovered with four different coring tools (a 3-m-hydraulic-piston corer (HPC), an "alien" rotary corer, and Livingstone and surface corers), modifications to the standard IODP methodology were required. In detailing this approach, we first outline the aims of the Junín Drilling Project and review the terminology used in the generation of a composite depth record and splice. We then detail the issues we encountered and the ways we addressed them, the development of the composite-depth scale and primary-stratigraphic splice, and discuss the advantages to be gained from integrating core images and visual core descriptions into this process. Finally, we use physical-property data acquired on the borehole during drilling to validate the complete-stratigraphic splice. These step-by-step descriptions and modifications will likely benefit future terrestrial and/or lacustrine deep-drilling projects and can serve as a template for those endeavors.

Site description

Lake Junín (11.03° S, 76.11°W) is a large (300 km²) semi-closed basin 4085 m above sea level in the Peruvian Andes (Seltzer et al. 2000; Rodbell et al. 2014) (Fig. 1). Although it has a large-surface area, it is relatively shallow (< 15 m water depth) and strongly sensitive to changes in regional water balance (precipitation/evaporation) driven by changes in the South American Summer Monsoon and the migration of the Intertropical Convergence Zone (Seltzer et al. 2000). Previous shallow coring efforts (< 20 m recovery) revealed that sediment accumulation in the lake alternates between the influx of clastic sediments during glacial periods and accumulations of authigenic calcite during interglacial periods. A geophysical site survey in 2011 revealed a potential sediment package >100 m thick that, coupled with sedimentation rates of 20–100 cm kyr⁻¹ over the past 50 ka (Wright 1980a), suggested Lake Junín could contain a sediment record spanning multiple glacial-interglacial cycles. As a result, the primary objective of the Lake Junín drilling project was to generate a long-continuous, high-resolution, and well-dated late Quaternary record of climate change for the tropical Andes.

Materials and methods

Coring operations

Eleven holes were cored across three sites in Lake Junín using a 3m HPC in August 2015. Here we focus exclusively on the sediments recovered from the five holes cored at Site 1, the longest record recovered from the central part of the lake at 8.5 m water depth (Fig. 1). Maximum penetration below lake-floor was 103.9 m in Hole A and cores from all holes yield quasi-continuous sediment records (Fig. 2). For the majority of operations, the hole was deepened in 3-m-increments irrespective of the length of the material recovered in order to better anticipate and cover minor coring gaps by offsetting the depths of subsequent holes. However, when recovery was less than 100%, stratigraphic gaps are created in the sediment record recovered from an individual hole (e.g. Hole A in Fig. 2). An alternative approach was adopted for the last five cores (31H to 35H) retrieved from Hole D (Fig. 2), where coring was advanced by recovery (i.e. the hole was deepened using the measured length of recovered core). This approach slowed coring operations but ensured fewer gaps existed between successive cores. Sediment recovery varied between boreholes but was significantly lower for Hole A (~72%) than for Holes B–E, which all exceeded 90% (Fig. 2). The recovered HPC cores were cut into ~1.5-m-long sections on the coring

platform, and, along with the core catcher, were curated following standard ICDP protocols using Expedition(including year)–Site and Hole–Core and Core Type–Section nomenclature (e.g. JUN15-1A-1H-1).

In addition to the HPC-cored sites, nine locations were shallow-cored (< 10 m penetration) in a NE–SW transect across the lake using a 1-m-Livingstone push-corer and a 1.5 m surface corer (Wright 1967; Weidhaas 2017). These shorter cores were obtained to capture the stratigraphic variability across the basin and to complement sampling of the uppermost few meters of soft sediment that is frequently more disturbed by the HPC (Melles et al. 2011; Ohlendorf et al. 2011). The Livingstone cores follow a Lake–Site and Year–Drive Number nomenclature (e.g. Junin-A15-D1) that is more widely used for this type of coring system. In contrast to the HPC system that progresses down a single hole at a site, successive Livingstone drives were offset laterally and overlapped by ~20 cm until the hole required casing (Wright 1980b); after casing, coring was advanced by the driven length of the previous core. We focus on cores from two of the nine sites, Junin-C15 and Junin-D15 (Fig. 2), that were cored in close proximity to each other and to Site 1 (Fig. 1). Site Junin-C15 consists of a surface core (0-0.91 meters below lake floor (mblf)) and 10 Livingstone drives to a depth of 7.72 mblf; the first six Livingstone cores overlap with each other (0.15–3.73 mblf). Site Junin-D15 consists of nine Livingstone drives that overlap between 0.65–4.31 mblf and extend down to 7.35 mblf (Fig. 2). The Junin-C15 surface core was extruded and sampled in 1 cm slices soon after recovery.

MS was measured on every recovered Livingstone and HPC whole core section in the field at 2.5-cm-intervals following recovery to inform drilling decisions and ensure complete recovery. Following completion of the field season, all HPC cores were shipped to the National Lacustrine Core Facility (LacCore) at the University of Minnesota for additional physical-property measurements, splitting, imaging, and long-term curation (Ohlendorf et al. 2011). Livingstone and surface cores were shipped to the University of Pittsburgh for similar analysis and curation.

Laboratory-based measurement of physical properties .

Whole-round HPC core sections were first measured on a Geotek multi-sensor core logger (MSCL) track system configured for GRA, MS, p-wave velocity (PWV), electrical resistivity (ER), and NGR at LacCore. GRA is a proxy for sediment density, PWV measures the sonic velocity of the sediment, MS is strongly

sensitive to the concentration of certain ferrimagnetic iron oxides, e.g. (titano)magnetite and maghemite, or occasionally iron sulfides, such as greigite, and NGR is a measure of radioactive isotopes, such as K, U, and Th, that emit gamma-rays. Measurements of GRA, PWV, and ER were made every 0.5 cm, and MS and NGR were measured every 4 cm. The first and last three GRA, PWV, and ER data points and the first and last MS and NGR data points in each core section were trimmed from the final dataset as the ends of cores are often influenced by volumetric-edge effects; unrealistic GRA values less than 0.5 g cm^{-3} , likely reflecting mm-scale gaps in the core, were also removed. Cores were then split and the archive halves were imaged using a high-resolution-line-scan camera using the LacCore standard operating procedure (SOP) settings for aperture, lighting, and focal distance; these settings were kept constant between core sections for the entire site to allow for direct comparison. Some cores contained darker sediments that were not adequately imaged using the SOP; for these cores a second, lighter, image was made to highlight variability in specific sections. Split-archive halves were then loaded onto a MSCL optimized for measurement of color reflectance (CR) using a color spectrophotometer (absorption bands ranged between 360-740 nm at 10 nm spacing) and point MS (MS_{point}) using a Bartington MS2E sensor; both of these parameters were measured at 0.5 cm spacing. All HPC core physical property datasets were processed and are archived at LacCore. The Livingstone cores were split and imaged at the University of Pittsburgh, and MS_{point} was measured at 0.2 cm spacing. All physical property measurement details can be found in ESM7.

Approach for generation of a composite depth record and stratigraphic splice

The primary stratigraphic splice from Lake Junín was accomplished by establishing a common depth scale for Junin-C15, Junin-D15, and the five holes at Site 1, and then by splicing together representative core sections from different drill sites/holes. This process involves several phases and within each phase there are opportunities for validation and refinement of both the composite-depth scale and splice. This approach is detailed in the “Junín Template” section of the manuscript and in Fig. 3, but first it is useful to define some key terms and review the methodological approaches that underpin this process.

A note on depth scales

In the process of building a composite-depth scale, we mainly refer to two depth scales, core-depth below-lake floor (CLF) and composite-core-depth-below-lake floor (CCLF); like many of the terms used here they are adapted from IODP terminology (IODP-MI 2011) (Table 1; ESM1). The CLF depth scale is equivalent to the more traditionally used meters-below-lake floor (mblf) depth scale, and is based on the drilling-depth-below-rig floor (DRF) depth scale, which is the sum of all the drill string component lengths measured beneath some datum on the rig floor, and the drilling-depth-below lake floor (DLF) depth scale, which uses the lake floor depth as a zero-point datum (Table 1; ESM1). The zero-depth point in the DLF depth scale is defined by the uppermost sediment in the first core, commonly referred to as the “mudline” core. A new DLF is defined for each subsequent core by adding the length that the drill string is advanced past the datum on the rig floor between coring. The CLF depth is based on the length of recovered core and the DLF; any point along the core is assigned a CLF based on the DLF plus the measured distance of that interval from the top of the core (Table 1; ESM1). The DLF depth scale can contain inaccuracies relating to platform heave and seasonal-to-daily variations in lake level (Rodbell et al. 2014), whereas the CLF depth scale can be influenced by the effects of core compression and expansion, coring deformation, and other sources of measurement error during drilling and/or curation. Sediment recovery is calculated as the length of recovered core relative to the interval cored and if sediment recovery exceeds 100%, which is often attributed to expansion and elastic rebound of the sediment (Moran 1997), then a secondary CLF depth scale (CLF-B; sometimes called a “compressed depth scale” or “scaled depth”) is routinely generated to prevent overlap in the CLF depth scale (IODP-MI 2011). The CLF-B depth scale employs a linear algorithm (Table 1) to compress the CLF depth to match the interval cored. However, as expansion is often not constant along the core and as the scaling is only arithmetic in nature, the CLF-B depth scale can cause offsets and errors if used directly during sampling. Thus, while we note the existence of this common alternate depth scale, we exclusively use the uncompressed CLF depth scale (CLF in Table 1) to generate the composite depth scale for Lake Junín.

The composite core below lake floor (CCLF) depth scale

When multiple holes are drilled at a site, inaccuracies in the CLF depth scale are often manifested as depth offsets between stratigraphically-equivalent features in different holes. The CCLF depth scale aims to correct for these inaccuracies by manipulating the CLF depth of individual cores to realign equivalent features in a common reference depth scale. This process begins with selection of the most

representative mudline core to define the top of the stratigraphic section and the zero-point-depth anchor in the CCLF depth scale. Cores are then iteratively tied into the composite depth scale by adding or subtracting a depth offset (a constant) to the whole core in order to align a single stratigraphically-equivalent point identified in both cores. These offsets can vary on a core-by-core basis and are tracked alongside the CLF depths in an affine table (ESM5). Cores are not stretched or squeezed to facilitate correlation but are instead “hung” next to each other to build the composite depth scale. It is not usually possible to align all potentially correlative features perfectly between two cores; in such cases, the offset is chosen to try to maximize correlations over the whole core. When correlations cannot be made across different holes due to ambiguities or gaps in stratigraphy, a core can be appended in the composite depth scale using the same CLF-CCLF offset as the core immediately above it. Subsequent cores are then correlated or appended to this core and the mapping of each core into the CCLF depth scale progresses from the mudline down through the deepest recovered cores.

Because of the non-destructive, high-resolution, and continuous nature of measurement coupled with the speed at which the data is obtained (Blum 1997), MSCL track data are the most frequently used datasets to identify equivalent features and correlate cores. However, whole-round MSCL data are strongly sensitive to variations in sediment volume that can result from cracks, voids, gaps, and/or coring disturbance so it is often necessary to augment these datasets with additional high-resolution-physical-property data acquired on the split cores e.g. XRF data (Evans et al. 2004; van Peer et al. 2017), color reflectance (Pälike et al. 2005), and/or high-resolution-line-scan imagery (Wilkens et al. 2013). By coupling these different datasets with detailed core descriptions, missing and/or disturbed intervals can be identified and/or omitted from the MSCL dataset prior to correlation (Evans et al. 2004; Ohlendorf et al. 2011; Wilkens et al. 2013). This multi-parameter approach reduces the potential for spurious matching compared to single-parameter-based correlations and offers a more robust approach to depth-scale construction and refinement. These are major factors that drive the revision of field-based-composite-depth scales and splices.

The down-section correlation of equivalent stratigraphic markers offers a more accurate approach than reliance on the drill string measurement. However, the CCLF depth scale is almost always expanded relative to the CLF depth scale and the mudline core is typically the only core in which the CLF and CCLF depths are the same. In marine sedimentary environments, this expansion (termed the growth factor) can often increase the CCLF scale by 5% to 20% relative to the CLF scale (Lisiecki and Herbert 2007; Hatfield 2015; van Peer et al. 2017). Although it is often difficult to identify the specific cause for

the growth factor, sources of expansion can arise from, but are not limited to: elastic rebound of the sediment (Moran 1997), depth errors during coring, stretching, squeezing, decompression and degassing of sediment after recovery, and decisions made during curation (Hagelberg et al. 1992; Mackillop et al. 1995; Pälike et al. 2005). Growth factors for lacustrine cores are typically lower than those observed in the marine realm, likely due to a combination of shallower water depths, shallower drilling, and shorter cores, though it is often difficult to find these reported. It is important to recognize and track any growth factor as the CCLF depth scale can yield higher estimates of sediment accumulation rate, and will be expanded relative to data acquired on the borehole during logging.

Splice Generation

Once the CCLF depth scale is established, intervals of different core sections are spliced together to generate a continuous- and complete-stratigraphic section. Splice points between cores use the same stratigraphically-equivalent-tie points that are used to generate the CCLF-depth scale to ensure that stratigraphy is neither missing nor repeated in the splice, and, in practice, the composite depth scale and splice are often built simultaneously using the most representative sections. However, because the selection of CLF-CCLF offsets between cores, splice tie points, and sections that comprise the “splice” are inherently subjective and dependent upon the operator, it is important that these decisions be as transparent and robust as possible. Splice points are listed using their section and interval identifiers alongside their CLF and CCLF depths in a splice table. It is important to note that the same composite depths of sediment sections in “off splice” sections may not necessarily represent the same stratigraphic interval of those “on splice”. Manual or automated (Lisiecki and Herbert 2007) correlation may be required to align equivalent specific off-splice intervals to the primary splice.

The Junín Template

We developed a multi-phase approach to generate the composite-depth scale and complete-stratigraphic splice that exploits the range of diverse datasets acquired through step-wise analysis of the Lake Junín cores (Fig. 3). First, a preliminary-composite-depth scale was developed in the field for the HPC cores using whole-round MS data; this provided a framework with which to base drilling decisions

(phase 1). Using these offsets as a starting point, we then used the laboratory-based whole-round MSCL datasets to query and refine the field-based composite-depth scale and generate a secondary CCLF-depth scale and splice using the Corewall Correlator software that is maintained and developed by the Continental Scientific Drilling Coordination Office (CSDCO) at the University of Minnesota (<https://csdco.umn.edu/resources/software/correlator>). Phase 2 is equivalent to the process used to construct composite-depth scales and splices on IODP expeditions that is reported in the IODP proceedings volume (Jaeger et al. 2014; Rosenthal et al. 2018). Next, to identify and replace correlations made using MSCL artifacts (e.g., cracks, voids), and further refine the composite-depth scale and splice, we evaluated every offset and splice tie point using the split-core data and high-resolution line-scan images (phase 3). This third layer of analysis offered an additional opportunity for refinement as the MSCL datasets can only provide correlative precision at the resolution they were acquired (0.5 - 4 cm for the HPC cores) whereas the line-scan images can potentially provide sub-millimeter-scale resolution for compositing and splicing. In some cases, the images were used to verify the MSCL tie points but in most instances they replaced and refined those made using the MSCL data. Once all tie points were verified and the composite depth scale and splice were finalized, we then returned to remap all off-splice cores into the revised CCLF depth scale using the MSCL datasets. This multiple-phase approach yields a rigorous methodology that allows for constant validation and fine-tuning of the composite-depth scale and splice through the introduction of additional multi-parameter higher-resolution data during each phase. As the phased approach outlined in Fig. 3 requires only standard MSCL, description, and imagery datasets, this template is easily transferrable to other projects.

Results

Physical property variability

Evaluation of the six MSCL datasets (GRA, MS, PWV, ER, NGR, and CR) revealed that MS, NGR, GRA, and CR (hereinafter presented as the lightness of the sediment; L^*) possessed the most reproducible variability to facilitate between-core and between-hole correlation (Fig. 4). GRA and L^* data contain high-frequency variability, particularly in the lower-value ranges, that is likely related to the greater sensitivity of these higher-resolution measurements (0.5 cm spacing) to small voids or cracks or lower-density gas-expanded sections. As the specific origin of each of these low values was not determined

they were not trimmed from the dataset, however, we did not use these GRA and L* intervals to facilitate between core correlations. Previous results from Lake Junín suggested that MS reflects the influx of lithogenic sediment eroded from the surrounding mountains predominantly to the east of the lake (Seltzer et al. 2000) (Fig. 1). MS data is consistent with this pattern, varying between low or negative values associated with authigenic carbonate and/or sections rich in organic material, and relatively high values in sections associated with higher clastic content (Fig. 4). NGR has a positive relationship with MS ($r = 0.48$; $n = 8241$; $p = < 0.0001$; Fig. 4), suggesting that lithogenic clays have higher concentrations of radioactive isotopes than authigenic carbonates or organic materials. GRA values increase with depth due to compaction, particularly below ~ 65 m, and along with L*, show much of the same longer-period, meter-scale variability as observed in MS and NGR (Fig. 4). Each of the four parameters contain intervals of variability that can be correlated across the different holes, but they also contain intervals of subtler variation where unambiguous matching of equivalent features is more difficult (Fig. 4). However, due to the diverse nature of these properties, when variability is low in one parameter, it is often higher in another parameter. For example, MS variability is relatively low between 20-25 m CLF but GRA and L* contain distinct features correlatable across three-different holes, and between 25-30 m CLF, GRA and L* variability decreases but MS variations are more distinct (Fig. 4). Where equivalent features are identified across different holes they appear slightly offset to one another (dashed lines in Fig. 4) and highlight depth inaccuracies in the CLF depth scale.

Correlating equivalent features

We demonstrate how equivalent stratigraphic features are correlated, assigned an offset in the CCLF depth scale, and how core sections are spliced together using the example of cores JUN15-1C-25H and JUN15-1E-16H (Fig. 5). A prominent MS peak in both cores (feature (i) in Fig. 5) permitted alignment of the two cores in the field, and with the addition of higher resolution MS_{point} , GRA, and L* data several other corresponding features confirm the stratigraphic equivalency of these two cores. We highlight one example from each dataset (features (i)-(iii) in Fig. 5) but several other intervals could have been chosen in each dataset to represent these features. Indeed, the subjective nature of selecting which dataset and datapoint to use to correlate two cores highlights the importance of documenting this process. Features (i), (ii), and (iii) are offset from each other by 10 cm, 11 cm, and 5 cm CLF, respectively (Fig. 5). The core images first provide visual confirmation of these pairings and are then used to determine an

unambiguous tie point between them at millimeter scale resolution. In this example the base of a thin black horizon, which also has pronounced GRA and L* expressions, was chosen at 75.238 m CLF in JUN15-1E-16H-2 and 75.178 m CLF in JUN15-1C-25H-2 (dashed lines in Fig. 5).

Alignment of this prominent MS peak in the CCLF depth scale requires the addition of 0.06 m to the CLF scale of core JUN15-1C-25H relative to core JUN15-1E-16H. As core JUN15-1E-16H has an existing offset of 1.367 m then the offset becomes 1.427 m for JUN15-1C-25H (ESM5). These features line up in the CCLF depth scale at a depth of 76.607 m CCLF, and the two cores are spliced together at this same juncture (Fig. 5; ESM6). Although the cores are aligned in the CCLF depth scale at this single point, the other equivalent MSCL features (features (i), (ii), and (iii) in Fig. 5) remain offset to one another by 4 cm, 5 cm, and -1 cm, respectively. This discrepancy is due to slight stratigraphic differences between the two cores and serves as a cautionary example as to why off-splice sections should not be transferred to on-splice depths by simply using the same offset determined between the CLF- and CCLF-depth scales.

A correction to the CLF depth scale

Correlation of features across different holes yields an additional opportunity to evaluate the DLF/CLF depth scale for potential errors. The DLF depths at the top of cores JUN15-1D-29H, JUN15-1D-30A, and JUN15-1D-31H are offset from one another in 3 m intervals; 81.08 m, 84.08 m, and 87.08 m, respectively. Cores JUN15-1D-29H and JUN15-1D-31H recovered 2.77 m and 2.60 m of sediment; core JUN15-1D-30A was drilled with the Alien tool, but recovered no sediment. MSCL data suggested, and core images confirmed, that the base of JUN15-1D-29H and the top of JUN15-1D-31H could be bridged with a single core section (JUN15-1C-28H-1) resulting in a 0.23 m CCLF gap between the two cores compared to the 3.23 m gap in the CLF depth scale (ESM2). To reconcile this 3 m difference, we suggest that after switching the drilling head from the HPC following JUN15-1D-29H to the Alien tool for JUN15-1D-30A, the drill string was mistakenly not advanced prior to coring operations. As the 81.08 – 84.08 m DLF interval had already been cored, and the Alien tool is a rotary coring system that is not designed for recovery of soft or in this case missing or disturbed sediment, this likely explains the lack of recovery for core JUN15-1D-30A. The coring apparatus was switched back to the HPC for core JUN15-1D-31H and the drill string was advanced 3 m to a DLF depth of 84.08 m, not the 87.08 m DLF as listed in the drilling log.

This explanation is consistent with the zero recovery of JUN15-1D-30A and with the -3 m difference in the CLF and CCLF depth scales between the two cores. As the DLF depth of subsequent cores is calculated from the DLF depth of the previous core plus drill string advancement, the 3 m DLF error was propagated downhole for the rest of the cores recovered from Hole D. Thus, cores JUN15-1D-31H through JUN15-1D-35H were corrected by -3 m in the CCLF depth scale in addition to any correlative adjustments made (Fig. 2; ESM5).

The CCLF depth scale and primary splice

The composite depth scale was constructed for Lake Junín cores between 0 and 104.272 m CCLF (ESM5). For the HPC cores the uppermost sediments (1 – 2 cores) were frequently more disturbed than the same interval recovered with the Livingstone corer making it difficult to unambiguously correlate the HPC cores and Livingstone cores using either the variability in the MSCL datasets or the core images. As a result, we omit the upper 1–2 HPC cores from each hole from the composite depth scale and incorporate the upper 6 – 7 m of the Livingstone record into the splice (ESM5, ESM6). To integrate sediments recovered with different coring systems, we initially developed separate CCLF depth scales for the HPC and Livingstone recovered cores. The two depth scales were then integrated using a single tie point at 6.665 m determined using both the MSCL data and the line scan images.

For three intervals it was necessary to append rather than correlate cores (ESM5); the reasons for appending these cores are: (i) cores JUN15-1A-34A, -35A, and -36H were the deepest recovered cores in the lake basin and do not overlap with cores retrieved from other holes; (ii) below 88.018 m CCLF, it was increasingly difficult to unambiguously correlate the cores recovered from Holes JUN15-1D and JUN15-1C. For cores JUN15-1D-32H through JUN15-1D-35H, coring was advanced by recovery to minimize between-core gaps so these cores are appended below core JUN15-1D-31H; (iii) the CCLF interval between 64.099 – 67.836 m contains three appended cores; JUN15-1C-21H, JUN15-1D-23H, and JUN15-1D-24H due to correlation ambiguities (ESM5). For the last of these three cores (JUN15-1D-24H), the CLF depth scale implied, and the MSCL data and high-resolution images confirmed, that the upper 71 cm of core section JUN15-1D-24H-1 recovered disturbed material from a previously cored interval. Therefore a depth of 71 cm in core JUN15-1D-24H-1 is used as the uppermost sediment horizon to append below core JUN15-1D-23H (ESM5). Appending cores does introduce discontinuities into the

CCLF scale, and potential gaps in the splice, but remains more faithful to the stratigraphy than the inclusion of potentially ambiguous tie points that may risk the repetition or removal of stratigraphy.

The splice incorporates the same tie points used to develop the CCLF-depth scale and was built simultaneously between 0–95.389 m CCLF; splice tie points are listed in ESM6. The splice is quasi-continuous (points ii and iii above), and the resulting spliced MS, NGR, GRA, and L* records show similar variations to each other and to changes in sediment color, which adds a qualitative degree of confidence to the splice. Sediment from hole JUN15-1D forms the backbone of the drill core splice; in the upper ~32 m CCLF, gaps between Hole JUN15-1D cores are frequently bridged using sediments from Hole JUN15-1B, between ~33–56 m CCLF Hole JUN15-1E cores are used, and between ~56–86 m CCLF sediments from Holes JUN15-1C and JUN15-1E are incorporated (Fig. 6; ESM6). Improvement of the CCLF depth scale over the CLF depth scale is illustrated through comparison of MS records from Holes JUN15-1C and JUN15-1D (ESM3). Without stretching or squeezing, it is not possible to align all MS features between holes, however, greater agreement between the two MS datasets in the CCLF depth scale ($r = 0.64$; $n = 2207$; $p < 0.0001$) compared to the CLF depth scale ($r = 0.43$; $n = 2207$; $p < 0.0001$), indicates greater alignment of equivalent features in the CCLF depth scale (ESM3). Growth factors (GF) are calculated for all holes ($GF = CCLF/CLF$; Table 1) and range between 0.9838 for Livingstone core Junin-D15 and 1.0193 for JUN15-1C (ESM4). Across all seven holes the average GF is 1.0167, representing an average 1.67% increase in the CCLF depth scale relative to CLF depth scale (ESM4).

Discussion

Splice and Borehole Comparison

To assess the representativeness of the splice we compare the splice MS record to the MS record acquired during the logging of boreholes JUN15-1A, JUN15-1C, and JUN15-1D (Pierdominici et al. 2016). The three borehole MS records are presented on the wireline log depth below lake floor (WLF) depth scale (Table 1; ESM1) and contain reproducible features across different holes at similar depths (Fig. 7). To account for the growth factor we present the splice MS data on the alternative CCLF-B depth scale ($CCLF-B = CCLF/GF$; Table 1). Splice MS features replicate the observations from holes A (purple), C (green), and D (blue) suggesting that the recovered sediments and the resulting splice from Lake Junín is

an accurate representation of sediment in the lake basin. Correlation between the MS borehole logs and the CCLF-B depth scale can be further improved through linear stretching and squeezing (Paillard et al. 1996) or by automated semi-quantitative matching of equivalent horizons (Lisiecki and Herbert 2007), whereas Monte Carlo-based correlations can add estimates of uncertainty (Malinverno 2013). However, while the CCLF-B depth scale likely yields a more accurate estimate of sediment accumulation rate, like the CLF-B depth scale it only provides an estimate of sediment thickness. As such, any reference to specific-depth intervals, such as that used for sampling, for refinement of the composite depth scale, or for generation of additional or alternate splices, should be made on the uncompressed CLF or CCLF depth scales.

Conclusions

ICDP drilling of Lake Junín recovered sediments using four separate coring systems to a depth of 103.9 m below the lake floor in August 2015. Using MSCL and imagery data acquired in the field and in the laboratory, we were able to correct errors in the CLF depth scale and develop, refine, and finalize the composite-depth scale and sediment splice for Site 1. The use of core imagery is not often incorporated into this process, but we showed that by making it an integral step in the process (Fig. 3, 5), we were able to robustly define the tie-points used in depth scale and splice construction at millimeter-scale resolution and a precision not obtainable with the MSCL datasets alone. The spliced MSCL data shows strong coherence with color variations in the sediment (Fig. 6) and with the MS data acquired during logging (Fig. 7), suggesting that the splice is an accurate representation of the sediment accumulated in the basin.

With a robust stratigraphic section established for Lake Junín, the primary age model can begin to be developed, research organized, and sampling undertaken along the splice aimed at addressing the bigger scientific questions of the Lake Junín Project. The value in detailing the stratigraphic correlation and splice construction makes these inherently subjective and 'black-box-esque' compositing and splice-development processes more transparent and traceable, thus making future revisions easier should they be required. For these reasons, we suggest that detailing this process should become a standard feature of future ICDP and terrestrial drilling projects, much like it has become on IODP expeditions. This manuscript and the approach detailed in Fig. 3 can potentially serve as a template for those endeavors.

Acknowledgements

This research was carried out with support from the U.S. National Science Foundation awards EAR-1400903 (Stoner), EAR-1404113 (Abbott), and EAR-1402076 (Rodbell) and from support by the ICDP, which in the US is operated out of the Continental Scientific Drilling Coordination Office (CSDCO) at the University of Minnesota. The Lake Junín Project would not have been possible without the team of drillers from DOESEC Exploration Services (USA), GEOTEC (Peru), and the expertise of Doug Schnurrenberger, Kristina Brady Shannon, and Mark Shapley of CSDCO. Logistical assistance was provided by Bryan Valencia, Angela Rozas-Davila, James Bartle, and Cecilia Oballe. RGH would like to thank Brian Grivna at the CSDCO for assistance with integrating the manually offset cores into LacCore-hosted software.

Author accepted manuscript

References

- Barker S, Chen J, Gong X, Jonkers L, Knorr G, Thornalley D (2015) Icebergs not the trigger for North Atlantic cold events. *Nature* 520: 333–336.
- Blake-Mizen KR, Hatfield RG, Stoner JS, Carlson AE, Xuan C, Walczak MH, Lawrence KT, Channell JET, Bailey I (2019) Southern Greenland glaciation and Western Boundary Undercurrent evolution recorded on Eirik Drift during the late Pliocene intensification of Northern Hemisphere glaciation. *Quaternary Sci Rev* 209: 40-51.
- Blum P (1997) *Physical Properties Handbook: A Guide to the Shipboard Measurement of Physical Properties of Deep-Sea Cores*. ODP Tech Note, 26.
- Channell JET, Hodell DA, Curtis JH (2016) Relative paleointensity (RPI) and oxygen isotope stratigraphy at IODP Site U1308: North Atlantic RPI stack for 1.2-2.2 Ma (NARPI-2200) and age of the Olduvai Subchron. *Quaternary Sci Rev* 131: 1-19
- Elderfield H, Ferretti P, Greaves M, Crowhurst S, McCave IN, Hodell D, Piotrowski AM (2012) Evolution of ocean temperature and ice volume through the Mid-Pleistocene Climate Transition. *Science* 337: 704-709.
- Evans HF, Westerhold T, Channell JET (2004) ODP Site 1092: Revised composite depth section has implications for Upper Miocene 'cryptochrons'. *Geophys J Int.* 156: 195-199.
- Hagelberg T, Pisias N, Shackleton N, Mix AC, Harris S (1995) Refinement of a high-resolution, continuous sedimentary section for studying equatorial Pacific Ocean paleoceanography, Leg 138. In: Pisias NG, Mayer LA, Janecek TR, Palmer-Julson A, and van Andel TH (Eds.), *Proc. ODP, Sci. Results 138, Ocean Drilling Program, College Station*, 31–46.
- Hagelberg T, Shackleton N, Pisias N, and Shipboard Scientific Party (1992) Development of composite depth sections for Sites 844 through 854. In: Pisias NG, Mayer LA, Janecek TR, Palmer-Julson A, and van Andel TH (Eds.) *Proc. ODP, Init. Repts. 138, Ocean Drilling Program, College Station*, 79–85.
- Hatfield RG (2015) Data report: stratigraphic correlation of Site U1396 and creation of a composite depth scale and splice. In: Le Friant A, Ishizuka O, Stroncik NA, and the Expedition 340 Scientists, *Proc. IODP 340, Integrated Ocean Drilling Program Management International, Inc., Tokyo*
- Herbert TD, Peterson LC, Lawrence KT, Liu Z (2010) Tropical ocean temperatures over the past 3.5 million years. *Science* 328: 1530–1534.
- Hernández-Molina FJ, Stow DA V, Alvarez-Zarikian CA, Acton G, Bahr A, Balestra B, Ducassou E, Flood R, Flores JA, Furota S, Grunert P, Hodell D, Jimenez-Espejo F, Kim JK, Krissek L, Kuroda J, Li B, Llave E, Lofi J, Lourens L, Miller M, Nanayama F, Nishida N, Richter C, Roque C, Pereira H, Sanchez-Goñi MF, Sierro FJ, Singh AD, Sloss C, Takashimizu Y, Tzanova A, Voelker A, Williams T, Xuan C (2014) Onset of Mediterranean outflow into the North Atlantic. *Science* 344: 1244–1250.
- IODP-MI (2011) IODP Depth Scales Terminology. <https://www.iodp.org/policies-and-guidelines/142-iodp-depth-scales-terminology-april-2011/file>

Jaeger JM, Gulick SPS, LeVay LJ, Asahi H, Bahlburg H, Belanger CL, Berbel GBB, Childress LB, Cowan EA, Drab L, Forwick M, Fukumura A, Ge S, Gupta SM, Kioka A, Konno S, Marz CE, Matsuzaki KM, McClymont EL, Mix AC, Moy CM, Muller J, Nakamura A, Ojima T, Ridgway KD, Rodrigues Ribeiro F, Romero OE, Slagle AL, Stoner JS, St-Onge G, Suto I, Walczak MH, Worthington LL (2014) Methods. In: Jaeger JM, Gulick SPS, LeVay LJ and the Expedition 341 Scientists, Proc. IODP 341, Integrated Ocean Drilling Program Management International, Inc., Tokyo

Kliem P, Enters D, Hahn A, Ohlendorf C, Lise-Pronovost A, St-Onge G, Wastegard S, Zolitschka B, the PASADO science team (2013) Lithology, radiocarbon chronology and sedimentological interpretation of the lacustrine record from Laguna Potrok Aike, southern Patagonia. *Quaternary Sci Rev* 71: 54–69.

Larsen HC, Saunders AD, Clift PD, Beget J, Wei W, Spezzaferri S (1994) Seven Million Years of Glaciation in Greenland. *Science* 264: 952–955.

Lisiecki LE, Herbert TD (2007) Automated composite depth scale construction and estimates of sediment core extension. *Paleoceanography* 22 PA4213.

Litt T, Anselmetti FS, Baumgarten H, Beer J, Cagatay N, Cukur D, Damci E, Glombitza C, Haug G, Heumann G, Kallmeyer J, Kipfer R, Krastel S, Kwiencien O, Meydan AF, Orcen S, Pickarski N, Randlett ME, Schmincke HU, Schubert CJ, Sturm M, Sumita M, Stockhecke M, Tomonaga Y, Vigliotti L, Wonik T, PALEOVAN Scientific Team (2012) 500,000 years of environmental history in Eastern Anatolia: The PALEOVAN Drilling project. *Sci. Drill.* 14: 18-29.

Mackillop AK, Moran K, Jarrett K, Farrell J, Murray D (1995) Consolidation properties of equatorial Pacific Ocean sediments and their relationship to stress history and offsets in the Leg 138 composite depth sections. In: Pias NG, Mayer LA, Janecek TR, Palmer-Julson A, and van Andel TH (Eds.), Proc. ODP, Sci. Results 138, Ocean Drilling Program, College Station, 357-369.

Malinverno A (2013) Data report: Monte Carlo correlation of sediment records from core and downhole log measurements at Sites U1337 and U1338 (IODP Expedition 321). In: Pälike H, Lyle M, Nishi H, Raffi I, Gamage K, Klaus A, the Expedition 320/321 Scientists, Proc. IODP 320/321, Integrated Ocean Drilling Program Management International, Inc., Tokyo

Melles M, Brigham-Grette J, Minyuk P, Koeberl C, Andreev A, Cook T, Fedorov G, Gebhardt C, Haltia-Hovi E, Kukkonen M, Nowaczyk N, Schwamborn G, Wennrich V, the El'gygytgyn Scientific Party (2011) The Lake El'gygytgyn scientific drilling project - conquering Arctic challenges through continental drilling. *Sci Drill.* 11, 29-40.

Melles M, Brigham-Grette J, Minyuk PS, Nowaczyk NR, Wennrich V, DeConto RM, Anderson AM, Andreev AA, Coletti A, Cook TL, Haltia-Hovi E, Kukkonen M, Lozhkin AV, Rosen P, Tarasov P, Vogel H, Wagner B (2012) 2.8 Million years of arctic climate change from Lake El'gygytgyn, NE Russia. *Science* 337: 315–320.

Moran K (1997) Elastic property corrections applied to Leg 154 sediment, Ceara Rise. In: Shackleton NJ, Curry WB, Richter C, and Bralower TJ (Eds.), Proc. ODP, Sci. Results 154, Ocean Drilling Program, College Station, 151-155.

- Ohlendorf C, Gebhardt C, Hahn A, Kleim P, Zolitschka B, the PASADO science team (2011) The PASADO core processing strategy - A proposed new protocol for sediment core treatment in multidisciplinary lake drilling projects. *Sediment Geol.* 239: 104-115.
- Paillard D, Labeyrie L, Yiou P (1996) Macintosh Program performs time-series analysis. *Eos, Trans. Amer. Geophys. Union* 77: 379–379
- Pälike H, Moore T, Backman J, Raffi I, Lanci L, Pares JM, Janecek T (2005) Integrated stratigraphic correlation and improved composite depth scales for ODP Sites 1218 and 1219. In: Wilson PA, Lyle M, Firth JV (Eds.) *Proc. ODP, Sci. Results 199, Ocean Drilling Program, College Station*, 1-41.
- Pierdominici S, Kück J, Rodbell DT, Abbott MB (2016) Preliminary analysis of downhole logging data from ICDP Lake Junin drilling Project, Peru. Presented at the EGU General Assembly 2016, 17-22nd April, Vienna, Austria. <http://adsabs.harvard.edu/abs/2016EGUGA..18.2291P>
- Praetorius SK, McManus JF, Oppo DW, Curry WB (2008) Episodic reductions in bottom-water currents since the last ice age. *Nat. Geosci.* 1: 449-452.
- Rodbell DT, Delman EM, Abbott MB, Besonen MT, Tapia PM (2014) The heavy metal contamination of Lake Junín National Reserve, Peru: An unintended consequence of the juxtaposition of hydroelectricity and mining. *GSA Today* 24: 4-10.
- Rosenthal Y, Holbourn AE, Kulhanek DK, Aiello IW, Babila TL, Bayon G, Beaufort L, Bova SC, Chun JH, Dang H, Drury AJ, Dunkley Jones T, Eichler PPB, Fernando AGS, Gibson K, Hatfield RG, Johnson DL, Kumagai Y, Li T, Linsley BK, Meinicke N, Mountain GS, Opdyke BN, Pearson PN, Poole CR, Ravelo AC, Sagawa T, Schmitt A, Wurtzel JB, Xu J, Yamamoto M, Zhang YG (2018) Expedition 363 methods. In Rosenthal Y, Holbourn AE, Kulhanek DK, and the Expedition 363 Scientists, *Western Pacific Warm Pool. Proceedings of the International Ocean Discovery Program, 363: College Station, TX*
- Ruddiman WF, Cameron D, Clement BM (1987) Sediment disturbance and correlation of offset holes drilled with the hydraulic piston corer: Leg 94. In: Ruddiman WF, Kidd RB, Thomas E et al. *Initial Reports DSDP 94. U.S. Govt. Printing Office, Washington* 615–634 doi:10.2973/dsdp.proc.94.111.1987
- Scholz CA, Cohen AS, Johnson TC, King J, Talbot MR, Brown ET (2011) Scientific drilling in the Great Rift Valley: The 2005 Lake Malawi Scientific Drilling Project — An overview of the past 145,000 years of climate variability in Southern Hemisphere East Africa. *Palaeogeog.r Palaeoclimatol. Palaeoecol.* 303: 3-19.
- Seltzer G, Rodbell D, Burns S (2000) Isotopic evidence for late Quaternary climatic change in tropical South America. *Geology* 28: 35-38.
- Stoner JS, Channell JET, Mazaud A, Strano SE, Xuan C (2013) The influence of high-latitude flux lobes on the Holocene paleomagnetic record of IODP Site U1305 and the northern North Atlantic. *Geochem. Geophys. Geosy.* doi: 10.1002/ggge.20272
- van Peer TE, Liebrand D, Xuan C, Lippert PC, Agnini C, Blum N, Blum P, Bohaty SM, Bown PR, Greenop R, Kordesch WEC, Leonhardt D, Friedrich O, Wilson PA (2017) Data report: revised composite depth scale and splice for IODP Site U1406. In Norris RD, Wilson PA, Blum P, and the Expedition 342 Scientists, *Proc. IODP 342: College Station, TX (Integrated Ocean Drilling Program)*

Weidhaas N (2017) A 25,000-year lake level history of Lake Junín, Peru from stratigraphic and oxygen isotope studies. Master's Thesis, University of Pittsburgh

Wilkens RH, Dickens GR, Tian J, Backman J (2013) Data report: revised composite depth scales for Sites U1336, U1337, and U1338. In: Pälike H, Lyle M, Nishi H, Raffi I, Gamage K, Klaus A, and the Expedition 320/321 Scientists, Proc. IODP, 320/321: Tokyo (Integrated Ocean Drilling Program Management International, Inc.).

Wright HE (1967) A square-rod piston sampler for lake sediments. *J. Sediment Res.* 37: 975-976.

Wright HE (1980a) Environmental History Of The Junín Plain And The Nearby Mountains. In: Rick JW (Ed) *Prehistoric Hunters Of The High Andes*. New York Academic Press, New York, 253–256

Wright HE (1980b) Cores of soft lake sediments. *Boreas* 9: 107–114

Zachos J, Pagani H, Sloan L, Thomas E, Billups K (2001) Trends, rhythms, and aberrations in global climate 65 Ma to present. *Science* 292: 686–693.

Zhang YG, Pagani M, Liu Z (2014) A 12-million-year temperature history of the tropical pacific ocean. *Science* 344: 84–87.

Author accepted manuscript

Figure Captions

Figure 1 Location of the Lake Junín drainage basin and the position of the three ICDP drill sites (yellow circles), the nine Livingstone core locations, and a piston core recovered in 1996 (Seltzer et al. 2000). Site 1 and Livingstone cores Junin-C15 and Junin-D15 are the focus of this manuscript.

Figure 2 Stratigraphic position of the two Livingstone-cored sites (Junin-C15 and Junin-D15) and the five HPC-cored sites (JUN15-1A through JUN15-1E) recovered from site 1 in Lake Junín. Core recovery for the HPC cores is calculated as the length of recovered core relative to the interval cored and expressed as a percentage. Hole D cores 31H through 35H are shown on the original CLF depth; the corrected CLF depths (see text and ESM2 for details) are shown alongside (denoted *) with the top and lower depths bracketed. Core recovery increases from 92.4% to 95.5% using the corrected CLF depth. Coring designations; Sfc. = Surface core, D = Livingstone Drive number, H = HPC core, A = Alien tool. Colors corresponding to each drill hole remain consistent for all remaining figures in this manuscript

Figure 3 Step-wise development (warm colors) of the composite-depth scale (CCLF) and stratigraphic splice for sediments recovered from Lake Junín; blue colors denote core flow, green colors denote acquisition of new data. The single-parameter MSCL MS record acquired in the field was used to generate a preliminary-CCLF depth scale to inform drilling decisions (phase 1). This preliminary-depth scale was refined using a multi-parameter whole-round MSCL dataset acquired in the laboratory and the splice was generated (phase 2). Both these records were then refined and finalized using the line-scan images, split-core MSCL datasets, and core description (phase 3). The splice was then utilized to guide working half sampling and age-model development to facilitate the scientific objectives of the Lake Junín drilling project, and can be used to interpret the data acquired on the borehole. MS – Magnetic Susceptibility; NGR – Natural Gamma Rays; PWV – P-Wave Velocity; GRA – Gamma Ray Attenuation Densitometry; ER – Electrical Resistivity; CR – Color Reflectance

Figure 4 MS, NGR, GRA, and L^* on the CLF depth scale for Holes A through E using the same colorations (JUN15-1A – purple; JUN15-1B – red; JUN15-1C – green; JUN15-1D – blue; JUN15-1E – orange) as utilized in Figure 2. The blue shading between 20-30 m highlights the region that is expanded to the right of the main dataset. In this expanded view, several equivalent features can be identified in the different physical properties (dashed lines), however, they are often offset in depth to each other, highlighting the inaccuracies in the CLF depth scale when comparing cores from different holes.

Figure 5 MS_{point} , (upper panels), GRA density (center panels) and L^* (lower panels) data shown on the CLF-depth scale (left) and the CCLF-depth scale (right) for core JUN15-1E-16H (orange) and core JUN15-1C-25H (green). Also shown are the high-resolution core images for core section JUN15-1E-16H-2 and JUN15-1C-25H-1. Three equivalent stratigraphic features can be identified between the two core sections in the MS_{point} (i), GRA (ii), and L^* (iii) datasets and one visual sediment contact has been highlighted (dashed lines). In the CLF depth scale, features a-c are offset from each other by 10 cm, 11 cm, and 5 cm, respectively; the dashed lines are offset by 6 cm (left panels). Validated by all four features, the sections are aligned using the visual correlation and are integrated into the CCLF depth scale (right panels) by shifting the depths of JUN15-1C-25H by +6 cm relative to JUN15-1E-16H-2. The sections are spliced at the same tie point; colored data are the on-splice intervals, grey data are off-splice intervals. Note that although on the CCLF-depth scale features (i), (ii), and (iii) remain offset to each other. This serves as an example as to why off-splice intervals cannot be assigned on-splice depths based on their CLF depth

Figure 6 Spliced MS, NGR, GRA, and L* records for the upper 95.39 m-CCLF of Lake Junín. Sections in the splice are color coded by the hole from which the data originates. The MSCL data are shown alongside the color profile generated from the spectrophotometer and show prominent shifts across all four property datasets associated with visible changes in sediment color and lithology

Figure 7 Splice MS record (black; left) on the CCLF-B-depth scale shown alongside the MS records acquired during logging of boreholes JUN15-1A (purple), JUN15-1C (green), and JUN15-1D (blue). The spliced-MS record is repeated (grey; not to scale) alongside each of the borehole records for comparison. The spliced MS record shows a striking similarity to the three borehole records, suggesting that the sediment splice generated for Lake Junín is strongly representative of the sediments accumulated in the basin

Author accepted manuscript

Table Captions:

Table 1: Summary and explanation of the drilling-depth scales used in the construction and discussion of the composite-depth scale and splice for Lake Junín.

Author accepted manuscript

Electronic Supplementary Material (ESM) Captions

ESM1: Depth-scale schematic showing the depths scales discussed in the text. A depth target can be measured directly using the drilling-below-rig floor (DRF) but is usually presented on the drilling-below-lake floor (DLF) depth scale that incorporates an estimate of both water depth and the offset between the datum on the rig floor and the water surface (D). The DRF minus the length of the mudline core can be used to estimate these two parameters. The core depth-below-lake floor (CLF) is calculated from the DLF at the top of the core plus the length of the interval measured into that core. The CLF at the core top and the DLF are the same value. Secondary CLF-B-, CCLF-, and CCLF-B-depth scales can be calculated from the CLF (Table 1). CCLF = core composite depth below lake floor; WRF = wireline depth below rig floor (WRF); WLF = wireline depth below lake floor (WLF) (Table 1)

ESM2: GRA data and high-resolution images for sections from cores JUN15-1D-29H, JUN15-1D-31H, and JUN15-1C-28H. The original CLF depth-scale suggested a 3.23 m gap exists between the base of JUN15-1D-29H-3 and the top of JUN15-1D-31H-1. Compositing and integration of these cores with data and images from core JUN-1C-28H suggests this gap is only 0.23 m and that a -3 m error exists in the CLF depth of core JUN15-1D-31H and all subsequent cores from Hole D. This is corrected in the CCLF depth scale and explained and justified in the text

ESM3: Comparison of MS records of Hole C and Hole D using the CLF-depth scale (upper panel) and CCLF-depth scale (lower panel). Comparisons are made between the two records by interpolating the Hole D data onto the respective Hole C CLF and CCLF depths. Note the stronger agreement between the two MS records on the CCLF depth scale that results from placing the data within a common depth reference

ESM4: CLF depth (m) vs CCLF depth (m) for all core tops from Holes A-E and in the lower right panel all seven holes together including Junin-C15 and Junin-D15. The growth factor (GF) is calculated as the expansion of the CCLF depth scale relative to the CLF scale and is expressed as a ratio and a percentage. The average GF for all holes is 1.0167 (1.67%)

ESM5: Core lengths, CLF depth, CCLF depth, offset between the CCLF and the CLF scales and the associated growth factor. Also noted are those cores that were not composited based on stratigraphy and those appended.

ESM6: Splice tie points on the CLF and CCLF depth scales for the primary stratigraphic splice from Lake Junín.

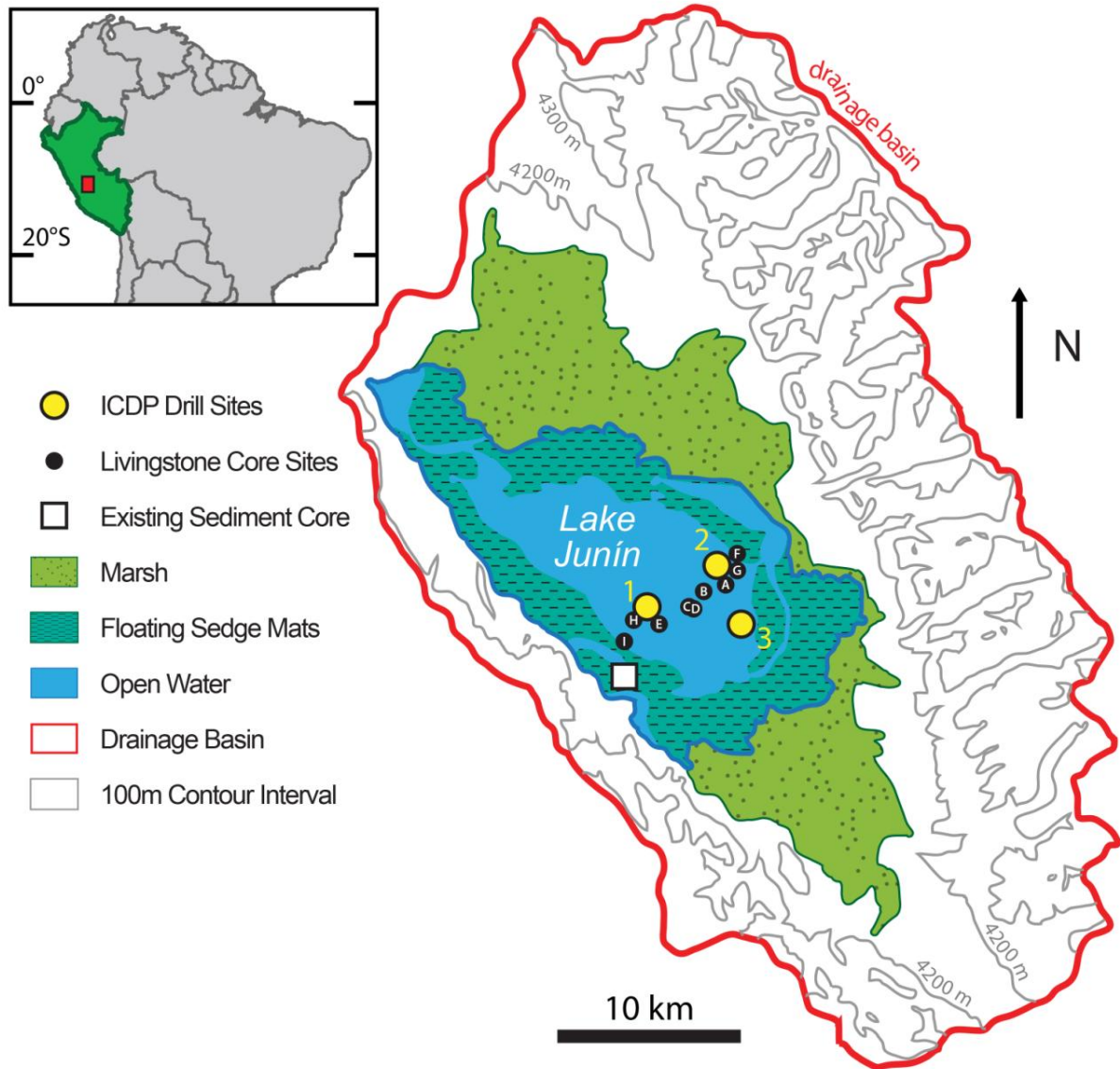
ESM7: Measurements, settings, and spacing used for the MSCL datasets used in the Lake Junín project

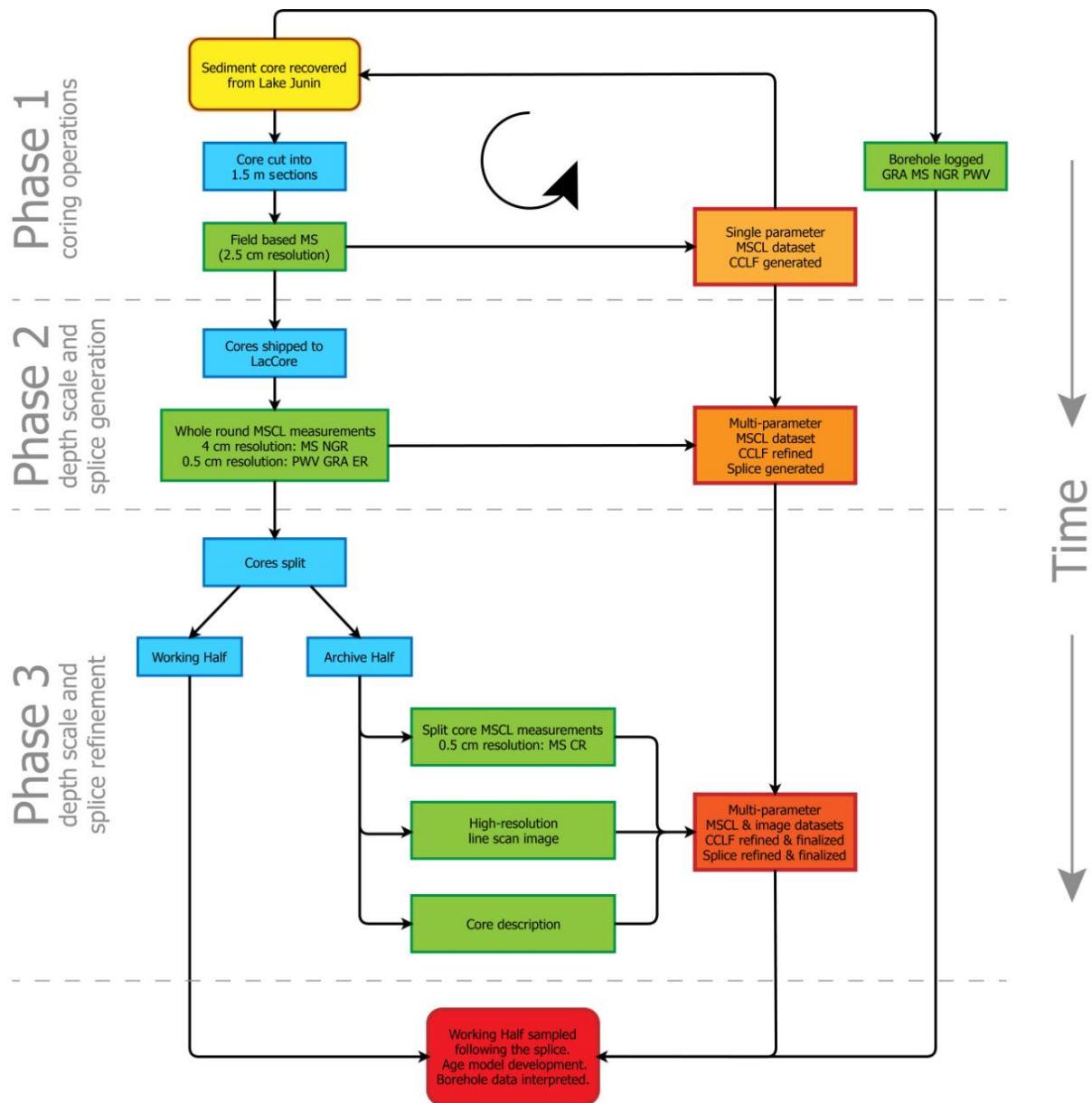
	Depth Name	Acronym	Datum	Description	Type
Drilling Depth Scale	Drilling Depth Below Rig Floor	DRF	Rig Floor	The sum of lengths of all drill string components deployed beneath the rig floor using the rig floor as the datum.	Measured depth
	Drilling Depth Below Lake Floor	DLF	Lake Floor	The length of all drill string components between the lake floor and target. [DLF = DRF – depth of lake floor below rig floor]	Processed Depth
Core Depth Scale	Core Depth Below Lake Floor	CLF	Lake Floor	Distance from lake floor to target within recovered core. [CLF = DLF + curated section length to target]	Processed Depth
	Core Depth Below Lake Floor	CLF-B	Lake Floor	Distance from lake floor to target within recovered core. This method applies a compression algorithm (i.e., scaling) if recovery is above 100%. [CLF-B = DLF + scaled (if necessary) curated section length to target]	Processed Depth
Composite Depth Scale	Core Composite Depth Below Lake Floor	CCLF	Lake Floor	Distance from lake floor to target within recovered core using a scale of adjusted depths constructed to resolve gaps in the core recovery and depth inconsistencies.	Composite Depth
	Compressed Core Composite Depth Below Lake Floor	CCLF-B	Lake Floor	This depth scale compresses the entire CCLF depth scale back to the depth of the drilled interval (based on the CLF depth scale) using the average growth factor (GF) where $GF = CCLF_{max}/CLF_{max}$ [CCLF-B = CCLF / GF]	Composite Depth

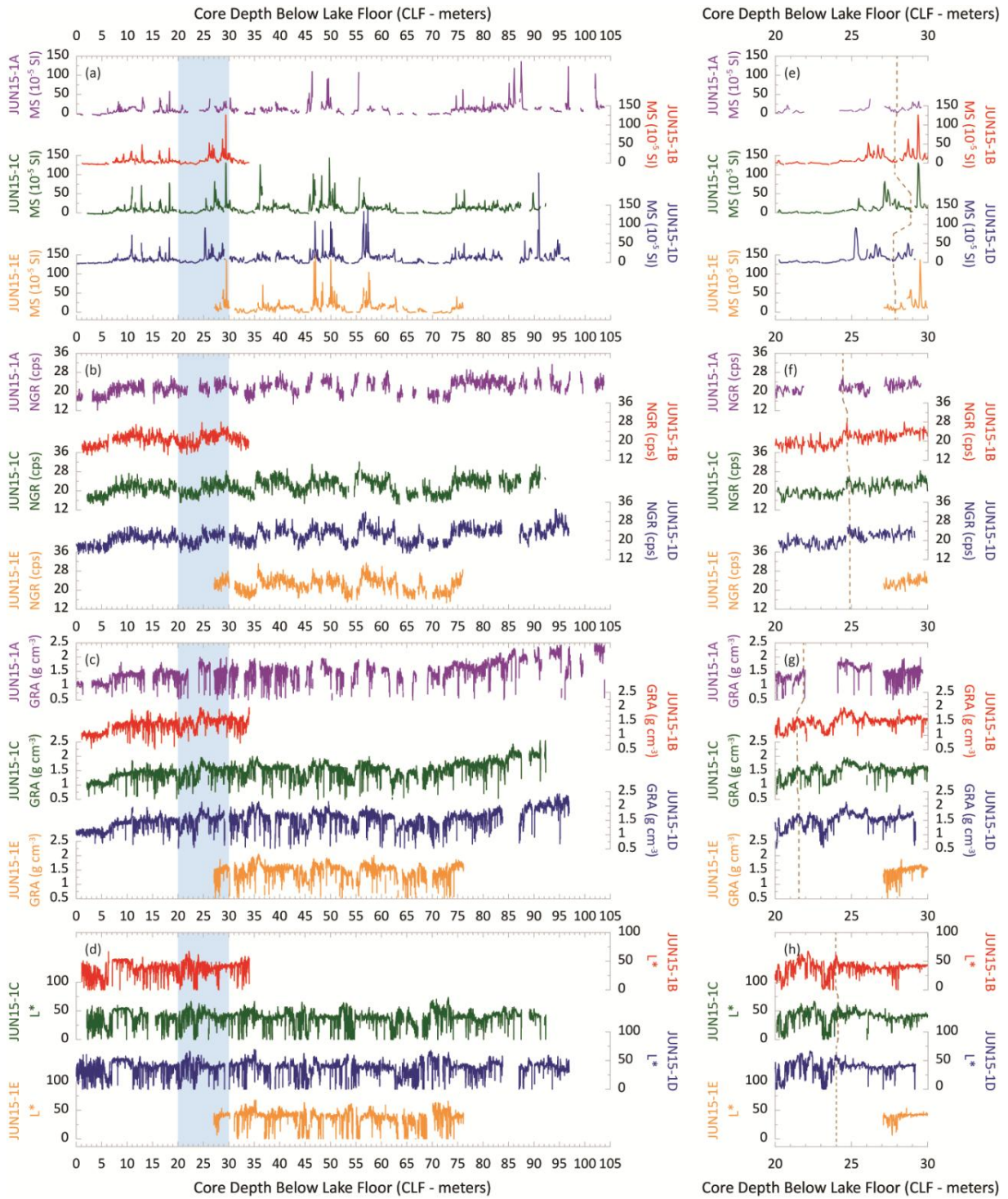
Wireline Depth Scale	Wireline Log	WRF	Rig Floor	Length of wireline and sensor offset between the rig floor and the target.	Measured Depth
	Depth Below				
	Rig Floor				
	Wireline Log	WLF	Lake Floor	WRF with lake floor depth below rig floor subtracted.	Processed Depth
	Depth Below				
	Lake Floor				

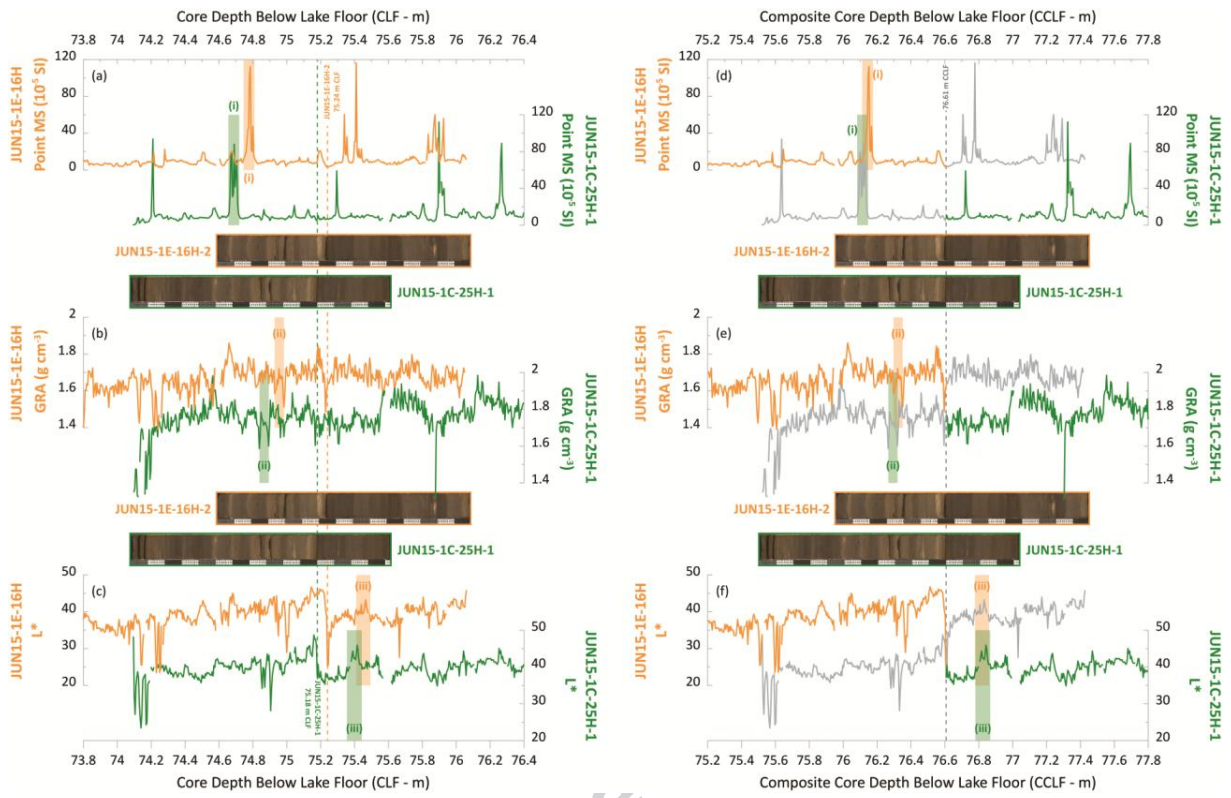
Table 1: Summary and explanation of the drilling depth scales used in the construction and discussion of the composite depth scale and splice for Lake Junín.

Author accepted manuscript

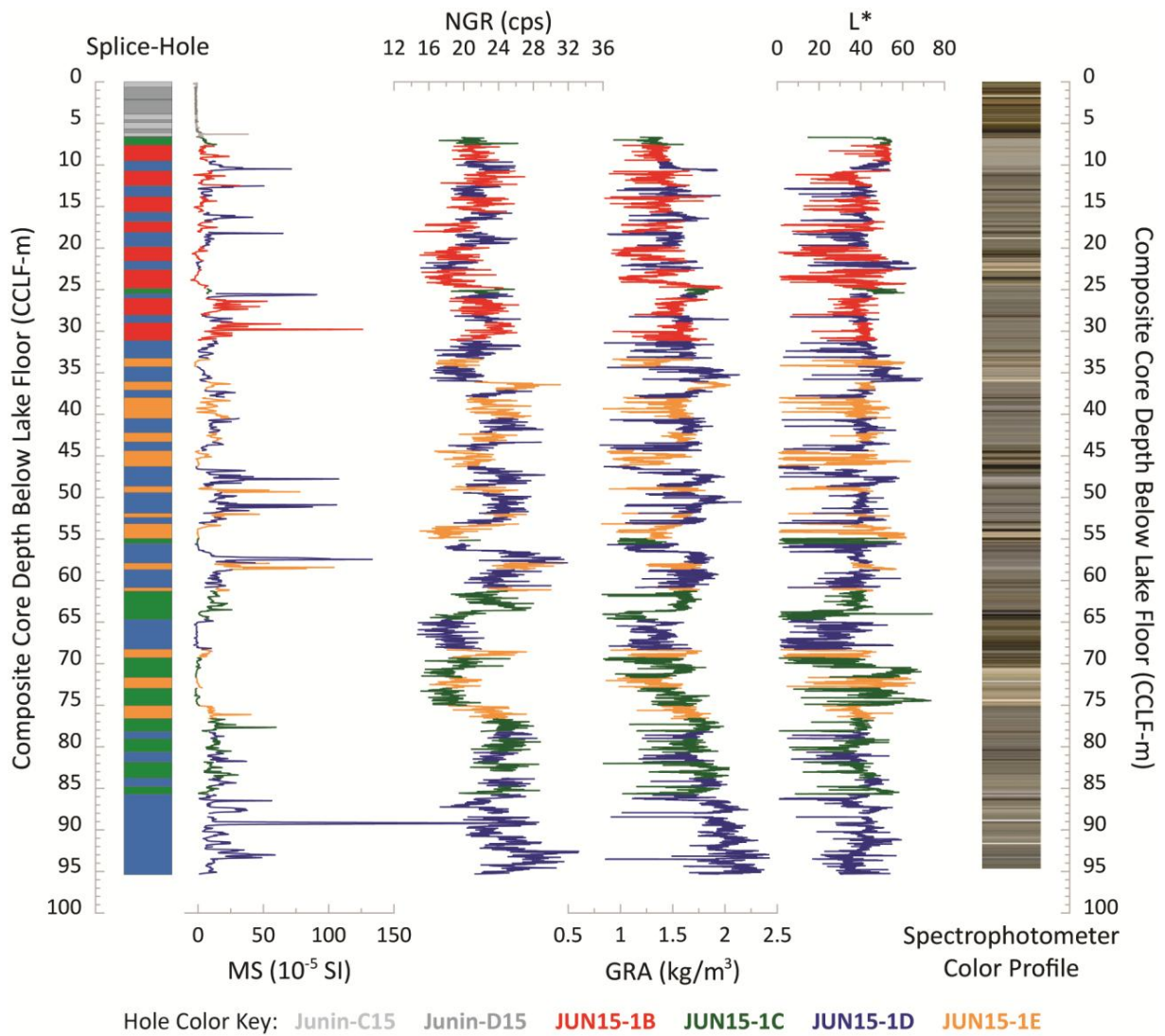








Author accepted



Authc